Paweł SZCZEŚNIAK, Zbigniew FEDYCZAK, Jacek KANIEWSKI

University of Zielona Góra, Institute of Electrical Engineering

Dynamic Model of a Space Vector Modulated Buck-Boost Matrix-Reactance Frequency Converter

Streszczenie. *Elementy pasywne w układzie Matrycowo-Reaktancyjnego Przemiennika Częstotliwości mają duży wpływ na jego parametry przy zmiennych wartościach zasilania lub obciążenia. Artykuł ten przedstawia dynamiczny model matematyczny Matrycowo-Reaktancyjnego Przemiennika Częstotliwości przy modulacji wektora przestrzennego napięcia wyjściowego (SVM). Metoda uśrednionych zmiennych stanu oraz dwuczęstotliwościowe przekształcenie d-q jest wykorzystane do opisu właściwości przekształtnika przy dynamicznych zmianach jego parametrów.* ***Model dynamiczny Matrycowo-Reaktancyjnego Przemiennika Częstotliwości****.*

Abstract*. The determination of the converter passive elements for various load and power grid conditions is of great importance to the proper operation of matrix-reactance frequency converters. This paper presents a novel dynamic model of a Matrix-Reactance Frequency Converter that utilizes a Space Vector Modulation (SVM) switching method. In this paper the average-state space method and the two-frequency d-q transformation are proposed as aids in the process of fast verification of the matrix-reactance frequency converter operation under specific dynamic conditions.*

Słowa kluczowe: Model matematyczny, Matrycowo-reaktancyjne przemienniki częstotliwości, Modulacja wektora przestrzennego.
Keywords: Mathematical model, matrix-reactance frequency converter, space vector modulation.

Introduction

The past few years have witnessed remarkable progress in research into direct power AC-AC frequency converters without a DC energy storage element [1]-[5]. The most common is the matrix converter (MC) [5], [6]. The major problem with frequency conversion without DC energy storage is the voltage transfer ratio - is less than one. In order to obtain a voltage gain greater than one, hybrid solutions have been proposed [1], [3]. Another group of AC-AC frequency converters with a buck-boost voltage transformation possibility and without DC energy storage are proposed in [2] and are called matrix-reactance frequency converters (MRFC). These topologies are based on the idea of connecting all of the unipolar PWM AC matrix-reactance choppers (MRC) with a direct matrix converter [7]. This approach makes it possible to obtain a load output voltage much greater than the source voltage. The family of MRFCs contains two topologies based on buck-boost, Ćuk, SEPIC and Zeta MRC and one topology based on the boost MRC. A similarly conception as that in [2] was proposed in [4]. The presented topology is a cascade connection of the AC MRC with buck-boost topology and a direct MC. It should be noted that in both MRFC solutions the electrical energy stored in the reactance elements during the period of input or output frequency is equal to zero, which is an essential difference in comparison to hybrid MCs.

The analysis and modelling of MRFC presents significant challenges, due to their discontinuous switching behaviour. Furthermore, given the increasing number of different modulation strategies, it is necessary to study their impact in converter dynamic operation. Previous papers have presented mathematical models of MRFCs with Venturini modulation [2], [8], [9]. This modulation is very simply and based on a low frequency modulation matrix. The SVM approach is based on the instantaneous space-vector representation of input and output voltages and currents [6]. The implementation of SVM into a MRFC control is presented in [10], [11]. The modulation waveforms in SVM are not given directly as in Venturini modulation, and depend on sectors which are located vectors of input current and output voltages. A second difficulty is the distortion of output line voltages [6], [15]. The output phase voltage measurements to point "N" are distorted but the line-to-line output voltages have sinusoidal shapes.

The main aim of this paper is to present mathematical dynamic models of the selected topologies of MRFCs with space vector modulation. One well-known approach to the modelling of PWM systems is to approximate their operation by averaging techniques [12]. The generalized averaging method is based on the fact that the waveforms can be approximated using a defined time interval. This interval in a MRFC is determined by a switching sequence period T_{Seq}. Initially, the average-state space method was widely used for DC-DC converter modelling. Then it was applied to other types of power converters: AC-DC, AC-DC-AC and AC-AC [12]-[13]. The analyzed circuit of the MRFC is modelled using the average-state space method. There are several analytical methods for obtaining averaged models. The modelling technique presented in this paper is based on solving mathematical differential equations [2], [9].

Analyzed matrix-reactance frequency converter

The MRFC based on MRC with buck-boost topology (MRFC-I-buck-boost), shown in Fig. 1, will be analyzed in this paper [2], [8]-[11].

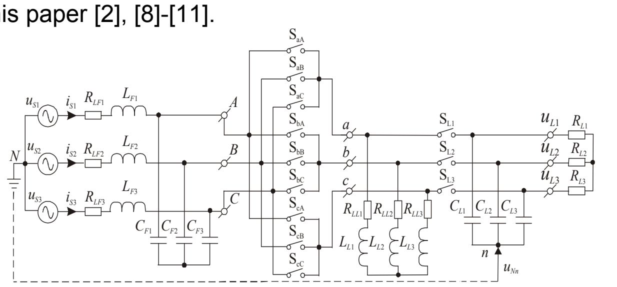

Fig. 1. Topology of Matrix-Reactance Frequency Converter based on matrix reactance chopper with buck-boost topology

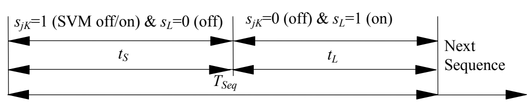

Fig. 2. General form of the control strategy

The descriptions, in general form, of the control strategies of the discussed MRFCs are shown in Fig. 2. In each switching cycle T_{Seq}, in the interval t_S, the matrix connected switch sets are in the process of switching with selected switching modulation, while the load synchronous connected switch sets are turned-off. In contrast, in the time period t_L all of the matrix connected switch sets are turned-off and the load switches are turned-on. The time interval t_L has an influence on the amplitude of load voltages. The state of the converter switches can be represented by means of the so-called transfer matrix $\mathbf{T}$:

$$(1)\quad \begin{bmatrix} u_a(t) \\ u_b(t) \\ u_c(t) \end{bmatrix} = \begin{bmatrix} s_{aA}(t) & s_{aB}(t) & s_{aC}(t) \\ s_{bA}(t) & s_{bB}(t) & s_{bC}(t) \\ s_{cA}(t) & s_{cB}(t) & s_{cC}(t) \end{bmatrix} \begin{bmatrix} u_A(t) \\ u_B(t) \\ u_C(t) \end{bmatrix} = \mathbf{T}\mathbf{u}_S\ ,$$

$$(2)\quad \mathbf{i}_S = \mathbf{T}^T \mathbf{i}_L\ .$$

The SVM technique is based on the instantaneous space vector representation of input and output voltages and currents. The output voltages and input currents of matrix connected switches in the presented MRFC can be expressed in its space phasor form as [6], [11]:

$$(3)\quad \underline{u}_{LMC} = \frac{2}{3}(u_a + u_b e^{j(2\pi/3)} + u_c e^{j(4\pi/3)}) = |u_{LMC}| e^{j\alpha_O}$$

$$(4)\quad \underline{i}_{SMC} = \frac{2}{3}(i_A + i_B e^{j(2\pi/3)} + i_C e^{j(4\pi/3)}) = |i_{SMC}| e^{j\beta_i}$$

where: α_o are the phase angles of the output voltage vector, β_i are the phase angles of the input current vector. The allowed switching configuration of matrix connected switches in the SVM algorithm are shown in Table I.

Table. 1. Switching configuration in the SVM algorithm

Switching Config.	a b c	u_{ab}, u_{bc}, u_{ca}	i_A, i_B, i_C	u_{LMC}	α_o	i_{SMC}	β_i
0_A	A A A	0 0 0	0 0 0	-	0	0	-
0_B	B B B	0 0 0	0 0 0	-	0	0	-
0_C	C C C	0 0 0	0 0 0	-	0	0	-
+1	A B B	u_{AB} 0 $-u_{AB}$	i_a $-i_a$ 0	$2/3u_{AB}$	0	$2/\sqrt{3}i_a$	$-\pi/6$
-1	B A A	$-u_{AB}$ 0 u_{AB}	$-i_a$ i_a 0	$-2/3\ u_{AB}$	0	$-2/\sqrt{3}i_a$	$-\pi/6$
+2	B C C	u_{BC} 0 $-u_{BC}$	0 i_a $-i_a$	$2/3u_{BC}$	0	$2/\sqrt{3}i_a$	$\pi/2$
-2	C B B	$-u_{BC}$ 0 u_{BC}	0 $-i_a$ i_a	$-2/3\ u_{BC}$	0	$-2/\sqrt{3}i_a$	$\pi/2$
+3	C A A	u_{CA} 0 $-u_{CA}$	$-i_a$ 0 i_a	$2/3u_{CA}$	0	$2/\sqrt{3}i_a$	$7\pi/6$
-3	A C C	$-u_{CA}$ 0 u_{CA}	i_a 0 $-i_a$	$-2/3\ u_{CA}$	0	$-2/\sqrt{3}i_a$	$7\pi/6$
+4	B A B	$-u_{AB}$ u_{AB} 0	i_b $-i_b$ 0	$2/3u_{AB}$	$2\pi/3$	$2/\sqrt{3}i_b$	$-\pi/6$
-4	A B A	u_{AB} $-u_{AB}$ 0	$-i_b$ i_b 0	$-2/3u_{AB}$	$2\pi/3$	$-2/\sqrt{3}i_b$	$-\pi/6$
+5	C B C	$-u_{BC}$ u_{BC} 0	0 i_b $-i_b$	$2/3u_{BC}$	$2\pi/3$	$2/\sqrt{3}i_b$	$\pi/2$
-5	B C B	u_{BC} $-u_{BC}$ 0	0 $-i_b$ i_b	$-2/3u_{BC}$	$2\pi/3$	$-2/\sqrt{3}i_b$	$\pi/2$
+6	A C A	$-u_{CA}$ u_{CA} 0	$-i_b$ 0 i_b	$2/3u_{CA}$	$2\pi/3$	$2/\sqrt{3}i_b$	$7\pi/6$
-6	C A C	u_{CA} $-u_{CA}$ 0	i_b 0 $-i_b$	$-2/3u_{CA}$	$2\pi/3$	$-2/\sqrt{3}i_b$	$7\pi/6$
+7	B B A	0 $-u_{AB}$ u_{AB}	i_c 0 $-i_c$	$2/3u_{AB}$	$4\pi/3$	$2/\sqrt{3}i_c$	$-\pi/6$
-7	A A B	0 u_{AB} $-u_{AB}$	0 i_c $-i_c$	$-2/3u_{AB}$	$4\pi/3$	$-2/\sqrt{3}i_c$	$-\pi/6$
+8	C C B	0 $-u_{BC}$ u_{BC}	$-i_c$ i_c 0	$2/3u_{BC}$	$4\pi/3$	$2/\sqrt{3}i_c$	$\pi/2$
-8	B B C	0 u_{BC} $-u_{BC}$	$-i_c$ 0 i_c	$-2/3u_{BC}$	$4\pi/3$	$-2/\sqrt{3}i_c$	$\pi/2$
+9	A A C	0 $-u_{CA}$ u_{CA}	0 $-i_c$ i_c	$2/3u_{CA}$	$4\pi/3$	$2/\sqrt{3}i_c$	$7\pi/6$
-9	C C A	0 u_{CA} $-u_{CA}$	i_c $-i_c$ 0	$-2/3u_{CA}$	$4\pi/3$	$-2/\sqrt{3}i_c$	$7\pi/6$

In Fig. 3 the output voltage and input current vectors corresponding to the 18 active configurations are shown. The complex space vector plane is divided into six sectors S_O for output voltages and six sectors S_i for source current. The reference output voltage and source current space-vectors are constructed by selecting four nonzero configurations (active vectors), applied to suitable time intervals within the switching sequence period T_{Seq}, as is determined by the equation (5)-(7), [6], [11]:

$$(5)\quad u_O = d_I u_I + d_{II} u_{II} + d_{III} u_{III} + d_{IV} u_{IV},$$

$$(6)\quad d_k = \frac{t_k}{T_{Seq}},\ k = \text{I, II, II, IV}, \qquad (7)\quad d_0 = 1 - d_I - d_{II} - d_{III} - d_{IV},$$

where u_I, u_{II}, u_{III} and u_{IV} are the output voltage vectors corresponding to the four selected configurations, and d_I, d_{II}, d_{III}, and d_{IV} are their duty cycles. The zero configurations are applied to complete time interval T_{Seq}.

Taking into account the switching time t_L of load switches (S_{L1}, S_{L2}, S_{L3}), and defining the sequence pulse duty factor $D_S = t_S/T_{Seq}$, the required modulation duty cycles for the switching configurations I, II, III, IV for MRFC from Fig. 1 are given by equations (8) - (11):

$$(8)\quad d_I = D_S(-1)^{S_0+S_i+1} \frac{2}{\sqrt{3}} q \frac{\cos(\alpha_0 - \pi/3)\cos(\beta_i - \pi/3)}{\cos\varphi_i},$$

$$(9)\quad d_{II} = D_S(-1)^{S_0+S_i} \frac{2}{\sqrt{3}} q \frac{\cos(\alpha_0 - \pi/3)\cos(\beta_i + \pi/3)}{\cos\varphi_i},$$

$$(10)\quad d_{III} = D_S(-1)^{S_0+S_i} \frac{2}{\sqrt{3}} q \frac{\cos(\alpha_0 + \pi/3)\cos(\beta_i - \pi/3)}{\cos\varphi_i},$$

$$(11)\quad d_{IV} = D_S(-1)^{S_0+S_i+1} \frac{2}{\sqrt{3}} q \frac{\cos(\alpha_0 + \pi/3)\cos(\beta_i + \pi/3)}{\cos\varphi_i},$$

where φ_i is the input phase displacement angle, α_O and β_i are the angles of the output voltage and input current vectors measured from the bisecting line of the corresponding sectors, and are limited as follows:

$$(12)\quad -\pi/6 < \alpha_0 < \pi/6, \qquad -\pi/6 < \beta_i < \pi/6 .$$

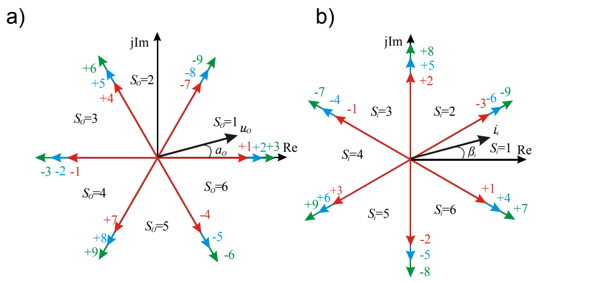

Fig. 3. Graphical interpretation of: a) sectors of the output voltage vectors, b) sectors of the input line current vectors

Modelling theory of MRFC

An average state-space model of MRFC is obtained when the following assumptions apply: - all the switches are ideal (the voltage drop across the diode when forward biased is zero, and there are no commutation losses in the transistor nor in the diode); - inductors and capacitors are linear; - converter and sources are symmetrical and balanced.

The local average of function $d(t)$ is defined as [13]:

$$(13)\quad d(t) = \frac{1}{T_{Seq}} \int_{t-T_{Seq}}^{t} q(\tau)d\tau\ ,$$

where: $d(t)$ is the continuous duty factor. For the next sequence periods T_{Seq} becomes $d(kT_{Seq}) = d_k(t)$, where $d_k(t)$ is the actual duty factor in the k-th cycle. If function $d(t)$ is periodic with period T_{Seq}, then $d(t) = D$ where D is the steady-state duty ratio [13]. The general form of the average state space equations is described by (14) [12].

$$(14)\quad \frac{d\overline{\mathbf{x}}}{dt} = \mathbf{A}(d)\overline{\mathbf{x}} + \mathbf{B}(d),$$

where: $\overline{\mathbf{x}}$ is the vector of the averaged state variables, $A(d)$ and $B(d)$ are the averaged state matrix and averaged input matrix respectively. The state-space averaging method is based on analytical manipulations using the different converter state representations [12]. This modelling technique consists in determining, firstly, the linear state model for each possible configuration of the circuit and, then, to combine all these elementary models into a single and unified one through a d_k duty factor.

$$\frac{d\mathbf{x}}{dt} = \mathbf{A}_k(t)\mathbf{x} + \mathbf{B}_k(t), \tag{15}$$

where: $\mathbf{x}$ are the vectors of the state variables; $\mathbf{A}_k(t)$ and $\mathbf{B}_k(t)$ are the state matrix and input matrix for *k-th* switch configuration respectively. The average state space equations for a MRFC can be represented by:

$$\frac{d\overline{\mathbf{x}}}{dt} = \mathbf{A}(d,t)\overline{\mathbf{x}} + \mathbf{B}(d,t), \tag{16}$$

$$\sum_{k=1}^{28} d_k = 1, \tag{17}$$

$$\mathbf{A}(d,t) = \sum_{k=1}^{28} d_k \mathbf{A}_k(d,t), \tag{18}$$

$$\mathbf{B}(d,t) = \sum_{k=1}^{28} d_k \mathbf{B}_k(d,t). \tag{19}$$

The weight coefficient d_k is the degree of occurrence of all the possible configurations, and depends on the switch control strategy. Equations (16) - (19) define the general form of the mathematical average state space model for MRFCs for various control strategies.

The model defined by equations (16) - (19) is time-varying model in state-space form, because the pulse duty factors d_k for MRFCs is a time variable [9]. A reduced time-invariant model of the MRFC can be found by expressing equations (16) in the *d-q* rotating frame using the two frequency transformation matrix:

$$\mathbf{K} = \begin{bmatrix} \mathbf{K}_S & \cdots & 0 \\ \vdots & \ddots & \vdots \\ 0 & \cdots & \mathbf{K}_L \end{bmatrix}, \tag{20}$$

where: $\mathbf{K}_S$ and $\mathbf{K}_L$ are the *d-q* transformation matrices defined for pulsation of the supply and load voltages, ω and ω_L respectively. Furthermore, assuming that the converter circuit is symmetrical and taking into consideration substitution (21) to (16) we obtain stationary time-invariant set equation (22) with new state variables [2], [9]:

$$\overline{\mathbf{x}} = \mathbf{KY}, \tag{21}$$

$$\frac{d\mathbf{Y}}{dt} = (\mathbf{A} - \mathbf{\Omega})\mathbf{Y} + \mathbf{B}, \tag{22}$$

A detailed matrix description for equations (22) is presented in reference [2]. The solution of the equation (22) is described by (23) [2].

$$\overline{\mathbf{x}} = \mathbf{K}e^{(\mathbf{A}-\mathbf{\Omega})t}\mathbf{Y}_0 + \mathbf{K}(\mathbf{A}-\mathbf{\Omega})^{-1}\left(e^{(\mathbf{A}-\mathbf{\Omega})t} - \mathbf{I}\right)\mathbf{B}, \tag{23}$$

where: $\mathbf{Y}_0$ – vector of the initial values of transformed variables, $\mathbf{I}$ – unit matrix. Equation (23) described a dynamic model of MRFC for different modulation.

Modelling of MRFC with SVM

Modelling process for MRFCs with SVM is based on the relationships described in Section III. Description of averaged state equations is connected with the calculation of averaged pulse duty factor for each switch S_{jK}, which is dependent on the SVM. Then, relationships between averaged values of voltages are described by (24).

$$\begin{bmatrix} \overline{u}_a \\ \overline{u}_b \\ \overline{u}_c \end{bmatrix} = \begin{bmatrix} d_{aA} & d_{aB} & d_{aC} \\ d_{bA} & d_{bB} & d_{bC} \\ d_{cA} & d_{cB} & d_{cC} \end{bmatrix} \begin{bmatrix} \overline{u}_A \\ \overline{u}_B \\ \overline{u}_C \end{bmatrix} = \mathbf{D}\overline{\mathbf{u}}_{ABC} \tag{24}$$

For example, in the sectors $S_i = 1$ and $S_O = 1$, the space vectors of voltages and currents are synthesized using the switch configurations +9, -7, -3, +1, which are defined in Tab. I. For the sequence: $+9 \rightarrow -7 \rightarrow -3 \rightarrow +1$ matrix switches are switched-on successively by a relative time:

$$|d_I| \rightarrow |d_{II}| \rightarrow |d_{III}| \rightarrow |d_{IV}|. \tag{25}$$

Then, the transformation matrix *D* is determined as follows:

$$\mathbf{D} = \mathbf{D}_{(+9)}|d_I| + \mathbf{D}_{(-7)}|d_{II}| + \mathbf{D}_{(-3)}|d_{III}| + \mathbf{D}_{(+1)}|d_{IV}|, \tag{26}$$

where:

(27)

$$\mathbf{D} = \begin{bmatrix} 1 & 0 & 0 \\ 1 & 0 & 0 \\ 0 & 0 & 1 \end{bmatrix}|d_I| + \begin{bmatrix} 1 & 0 & 0 \\ 1 & 0 & 0 \\ 0 & 1 & 0 \end{bmatrix}|d_{II}| + \begin{bmatrix} 1 & 0 & 0 \\ 0 & 0 & 1 \\ 0 & 0 & 1 \end{bmatrix}|d_{III}| + \begin{bmatrix} 1 & 0 & 0 \\ 0 & 1 & 0 \\ 0 & 1 & 0 \end{bmatrix}|d_{IV}|$$

Finally, the matrix *D* has the form (28).

$$\mathbf{D} = \begin{bmatrix} |d_I| + |d_{II}| + |d_{III}| + |d_{IV}| & 0 & 0 \\ |d_I| + |d_{II}| & |d_{IV}| & |d_{III}| \\ 0 & |d_{II}| + |d_{IV}| & |d_I| + |d_{III}| \end{bmatrix}. \tag{28}$$

In the averaged mathematical model of the MRPC with SVM voltage u_{Nn} (Fig. 1) should be considered in the equations and is described by expressions (29) [10].

$$\overline{u}_N = \frac{\left(\overline{u}_a + \overline{u}_b + \overline{u}_c\right)}{3} \tag{29}$$

Taking into account the equation (24) finally yields:

$$\overline{u}_N = s_1\overline{u}_A + s_2\overline{u}_B + s_3\overline{u}_C, \tag{30}$$

where:

$$s_1 = \frac{d_{aA} + d_{bA} + d_{cA}}{3}, s_2 = \frac{d_{aB} + d_{bB} + d_{cB}}{3}, s_3 = \frac{d_{aC} + d_{bC} + d_{cC}}{3}$$

Taking into account the equations (24) - (30) yields the final form of the averaged state space model (16) of the converter shown in Fig. 1 with SVM described by (31).

(31)

$$\begin{bmatrix} \frac{d\overline{i}_{S1}}{dt} \\ \frac{d\overline{i}_{S2}}{dt} \\ \frac{d\overline{i}_{S3}}{dt} \\ \frac{d\overline{i}_{LS1}}{dt} \\ \frac{d\overline{i}_{LS2}}{dt} \\ \frac{d\overline{i}_{LS3}}{dt} \\ \frac{d\overline{u}_{CF1}}{dt} \\ \frac{d\overline{u}_{CF2}}{dt} \\ \frac{d\overline{u}_{CF3}}{dt} \\ \frac{d\overline{u}_{L1}}{dt} \\ \frac{d\overline{u}_{L2}}{dt} \\ \frac{d\overline{u}_{L3}}{dt} \end{bmatrix} = \begin{bmatrix} -\frac{R_{LF1}}{L_{F1}} & 0 & 0 & 0 & 0 & 0 & -\frac{1}{L_{F1}} & 0 & 0 & 0 & 0 & 0 \\ 0 & -\frac{R_{LF2}}{L_{F2}} & 0 & 0 & 0 & 0 & 0 & -\frac{1}{L_{F2}} & 0 & 0 & 0 & 0 \\ 0 & 0 & -\frac{R_{LF3}}{L_{F3}} & 0 & 0 & 0 & 0 & 0 & -\frac{1}{L_{F3}} & 0 & 0 & 0 \\ 0 & 0 & 0 & -\frac{R_{LS1}}{L_{S1}} & 0 & 0 & \frac{d_{aA}-s_1}{L_{S1}} & \frac{d_{aB}-s_2}{L_{S1}} & \frac{d_{aC}-s_3}{L_{S1}} & \frac{(1-D_S)}{L_{S1}} & 0 & 0 \\ 0 & 0 & 0 & 0 & -\frac{R_{LS3}}{L_{S3}} & 0 & \frac{d_{bA}-s_1}{L_{S2}} & \frac{d_{bB}-s_2}{L_{S2}} & \frac{d_{bC}-s_3}{L_{S2}} & 0 & \frac{(1-D_S)}{L_{S2}} & 0 \\ 0 & 0 & 0 & 0 & 0 & -\frac{R_{LS3}}{L_{S3}} & \frac{d_{cA}-s_1}{L_{S3}} & \frac{d_{cB}-s_2}{L_{S3}} & \frac{d_{cC}-s_3}{L_{S3}} & 0 & 0 & \frac{(1-D_S)}{L_{S3}} \\ \frac{1}{C_{F1}} & 0 & 0 & -\frac{d_{aA}}{C_{F1}} & -\frac{d_{bA}}{C_{F1}} & -\frac{d_{cA}}{C_{F1}} & 0 & 0 & 0 & 0 & 0 & 0 \\ 0 & \frac{1}{C_{F2}} & 0 & -\frac{d_{aB}}{C_{F2}} & -\frac{d_{bB}}{C_{F2}} & -\frac{d_{cB}}{C_{F2}} & 0 & 0 & 0 & 0 & 0 & 0 \\ 0 & 0 & \frac{1}{C_{F3}} & -\frac{d_{aC}}{C_{F3}} & -\frac{d_{bC}}{C_{F3}} & -\frac{d_{cC}}{C_{F3}} & 0 & 0 & 0 & 0 & 0 & 0 \\ 0 & 0 & 0 & -\frac{(1-D_S)}{C_{L1}} & 0 & 0 & 0 & 0 & 0 & -\frac{1}{R_1C_{L1}} & 0 & 0 \\ 0 & 0 & 0 & 0 & -\frac{(1-D_S)}{C_{L2}} & 0 & 0 & 0 & 0 & 0 & -\frac{1}{R_2C_{L2}} & 0 \\ 0 & 0 & 0 & 0 & 0 & -\frac{(1-D_S)}{C_{L3}} & 0 & 0 & 0 & 0 & 0 & -\frac{1}{R_3C_{L3}} \end{bmatrix} \begin{bmatrix} \overline{i}_{S1} \\ \overline{i}_{S2} \\ \overline{i}_{S3} \\ \overline{i}_{LL1} \\ \overline{i}_{LL2} \\ \overline{i}_{LL3} \\ \overline{u}_{CF1} \\ \overline{u}_{CF2} \\ \overline{u}_{CF3} \\ \overline{u}_{L1} \\ \overline{u}_{L2} \\ \overline{u}_{L3} \end{bmatrix} + \begin{bmatrix} u_{S1} \\ u_{S2} \\ u_{S2} \\ 0 \\ 0 \\ 0 \\ 0 \\ 0 \\ 0 \\ 0 \\ 0 \\ 0 \end{bmatrix}$$

Validation of MRFC dynamic model

Two different models of the system in Fig. 1 are developed and analysed in the Matlab Simulink software environment. In one model the MRFC is represented by equations (22) and (31), and is referred to as the averaged model. In the second model (simulation model), the MRFC is represented by ideal switches and referred to as the exact model. The parameters used in both models are the same (Tab. II). It should be noted that distortions due to switching phenomena and its associated harmonics are generally observable in the waveforms obtained from the simulation model. The switching distortion is not present in the averaged model. To provide a meaningful comparison of the exact model and the average model, the corresponding time waveforms obtained from both models are juxtaposed in one graph. As an example, let us apply the obtained averaged model to modelling MRFCs in a step change of the D_S in time t_0. The transient responses of source current and load voltage at a step change of the D_S from 0.5 to 0.7, for f_L=25Hz, are presented in Fig. 4. The obtained results confirm that averaged models can be useful for transient response analysis of the described MRFC. The waveforms in Fig. 4 confirm the good dynamic properties of such a converter. The converter transient response is relatively short. The transient period is approximately equal to 0.25 times the supply period. Fig. 5 shows the system responses to the changes of f_L from 50 to 20 Hz. The corresponding results from both models agree very well with and validate the accuracy of the averaged model versus the exact model. The calculation and simulation test results demonstrate good correlation.

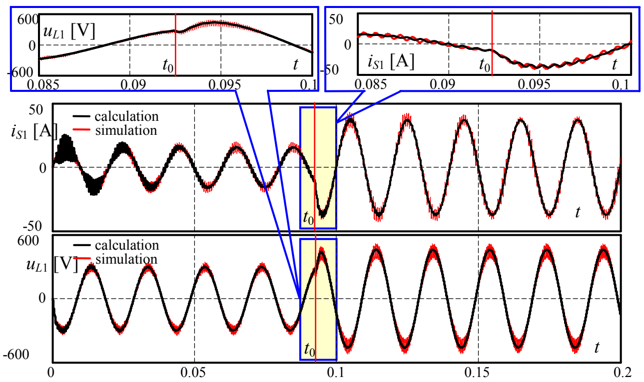

Fig. 4. Transient responses of input current and output voltage at step change of D_S from 0.5 to 0.75, f_L=25Hz

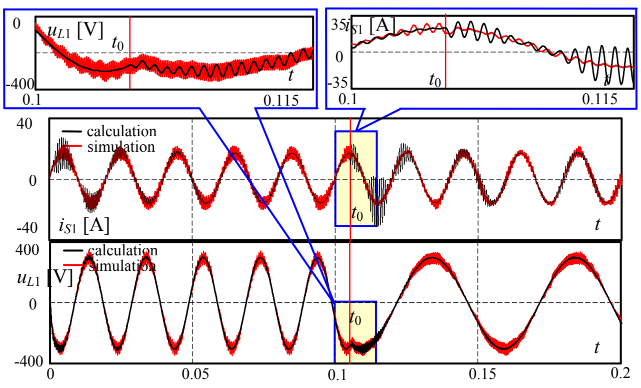

Fig. 5. Transient responses of input current and output voltage at step change of f_L from 50 to 20 Hz, D_S=0.6

Tab. 2. Calculation and simulation test circuit parameters

Parameter	Symbol	Calc./Simul.
Supply voltage frequency	U_S/f	230 V/ 50 Hz
	L_{F1} - L_{F3}	1.5 mH
Inductances	L_{L1} - L_{L3}	1.5 mH
Capacitances	C_{F1} - C_{F3}	10 μF
	C_{L1} - C_{L3}	10 μF
Load	R_{L1} – R_{L3}	60 Ω

Conclusion

Due to the fact that MRFCs are novel converters, before experimental verification it is necessary to examine their basic properties especially in dynamic conditions. The obtained models are a key tool in the study of low dynamic behaviour. In this paper, the theoretical test results have been compared with the results obtained by simulation. Based on the obtained results it can be concluded that MRFC have good dynamic properties.

The modelling approach based on the averaged state space method presented in this paper is relatively simple and requires only a small number of mathematical transformations. Comparative studies of the theoretical results and the results of simulation investigations have demonstrated the usefulness and accuracy of the obtained mathematical models.

Acknowledgments

The project has been funded by the National Science Centre granted on the basis of decisions number DEC-2011/03/B/ST8/06214.

REFERENCES

[1] Kolar J.W., Friedli T., Krismer F., Round S.D., The essence of three-phase AC/AC converter systems, EPE-PEMC'08, Poznań, Poland, (2008), 27–42

[2[Fedyczak Z., Szcześniak P., Korotyeyev I., New family of matrix-reactance frequency converters based on unipolar PWM AC matrix-reactance choppers, *Int. Power Electronics and Motion Control Conference* (*EPE-PEMC'08*), Poznań, Poland, (2008), 236–243.

[3] Klumpner C., Pitic C., Hybrid matrix converter topologies: an exploration of benefits, PESC'08, Rhodes, Greece, (2008), 2–8

[4] Koiwa K., Itoh J-i, Experimental verification for a matrix converter with a V-connection AC chopper, EPE'11, Birmingham, UK, (2011), 1–10

[5] Kolar J.W., Friedli T., Rodriguez J., Wheeler P.W., Review of three-phase PWM AC–AC converter topologies, *IEEE Trans. Ind. Electron.*, 58 (2011) n.11, 4988–5006

[6] Rodriguez J., Rivera M., Kolar J.W., Wheeler P.W., A review of control and modulation methods for matrix converters, *IEEE Trans. Ind. Electron.*, 59 (2012), n.1, 58–70

[7] Fedyczak Z., Strzelecki R., Sozański K., Review of three-phase AC/AC semiconductor transformer topologies and applications, *SPEEDAM'02*, Ravello, Italy, 2002.

[8] Szcześniak P., Fedyczak Z., Klytta M., Modeling and analysis of a matrix-reactance frequency converter based on buck–boost topology by DQ0 transformation, *Int. Power Electronics and Motion Control Conference* (*EPE-PEMC'08*), Poznań, Poland (2008) 165–172

[9] Szcześniak P., Fedyczak Z., Matrix-reactance frequency converters using an low frequency transfer matrix modulation method, *Electric Power Systems Research*, 83 (2012) n.1, 91-103

[10]Fedyczak Z., Szcześniak P., Tadra G., Klytta M., A comparison of basic properties of the integrated and cascade matrix-reactance frequency converters, *Int. Power Electronics and Motion Control Conference* (*EPE-PEMC'12*), Novi Sad, Serbia, Sept. (2012)

[11]Middlebrook R.D., Ćuk S., A general unified approach to modelling switching-converter power stages, PESC'76, (1976), 73–86

[12]Rim C.T, Hu D.Y, Cho G.H., Transformers as equivalent circuits for switches: general proofs and D-Q transformation-based analyses, *IEEE Trans. Ind. Appl.*, 26 (1990), n.4, 777-785

[13]Maksimovic D., Stankovic A.M., Thottuvelil V.J., Verghese G.C., Modeling and simulation of power electronic converters, *Proc. IEEE*, 89, (2001) n.6, 898-912

Autorzy: *dr hab. inż. Zbigniew Fedyczak, prof. UZ, dr inż. Paweł Szcześniak, dr inż. Jacek Kaniewski, Uniwersytet Zielonogórski, Instytut Inżynierii Elektrycznej, ul. Podgórna 50, 65-246 Zielona Góra, E-mail: Z.Fedyczak@iee.uz.zgora.pl, P.Szczesniak@iee.uz.zgora.pl, J.Kaniweski@iee.uz.zgora.pl.*